Precise Point Positioning with Ionospheric-Free Deviation Mask under Ionospheric Scintillation in Equatorial Region

Nguyen Viet Khoi[1,2]*, La The Vinh[1]

[1]*Hanoi University of Science and Technology, Ha Noi, Vietnam*
[2]*Polytechnic University of Catalonia, Barcelona, Spain*
**Corresponding author email: viet.khoi.nguyen@upc.edu*

Abstract

One of the most challenging phenomena threatening the performance of satellite navigation services is ionospheric scintillation, characterized by rapid fluctuation in the amplitude and phase of the received radio signals. Although scintillation in high-latitude regions is mostly caused by refractive effect which can be eliminated by dual-frequency measurements, the non-dispersive diffractive effect experienced in low-latitude region is still hazardous. This paper introduces an improvement into Precise Point Positioning (PPP) using a cycle-slip corrector based on ionosphere-free (IF) combination and a satellite mask based on a recently introduced scintillation index called Sigma-IF for dual-frequency conventional receivers. A comparison with the index from the standard deviation of geometry-free (GF) combination is made and analyzed. A significant improvement in accuracy and continuity of PPP after applying the proposed method is presented in the results obtained from well-known IGS stations. The increasing number of dual-frequency Global Navigation Satellite Systems (GNSSs) receivers launched into the mass market is a promising enhancement to the integrity of location-based applications.

Keywords: Ionospheric scintillation, Precise Point Positioning, Global Navigation Satellite System (GNSS).

1. Introduction

Recently, positioning solutions using Global Navigation Satellite System (GNSS) have been widely developed offering high accuracy and integrity. Taking advantage of carrier-phase measurements and precise ephemeris provided by the International GNSS Service (IGS) [1] as well as the Automatic Precise Positioning Service (APPS) [2] as detailed in Table 1, Precise Point Positioning (PPP) can achieve an accuracy up to few centimetres. The availability of real-time precise satellite orbit and clock products paves the way for real-time PPP.

Ionospheric effects have a detrimental impact on the propagation of GNSS radio signals and the performance of PPP services. Indeed, ionospheric irregularities can refract and diffract the signals causing rapid fluctuations of signal amplitude and/or carrier-phase, called ionospheric scintillation. This phenomenon results in significantly noisy carrier-phase observables, frequent cycle-slips [3] and losses of lock in the tracking loop. In such circumstances, the stability and precision of PPP are endangered as a result of the decreasing number of satellites.

On one hand, ionospheric refraction is associated with remarkable carrier-phase fluctuations but moderate signal amplitude fluctuations [4]. Applied in PPP, the dual-frequency ionosphere-free (IF) combination, denoted L_{IF}, can cancel out up to 99.9%

of the refraction [5, 6]. Ionospheric scintillation at high latitudes is mainly made up of refractive scintillation and thus, the IF-combination-based PPP is able to deliver the same accuracy level of navigation as under quiet ionospheric condition [3].

On the other hand, equatorial regions usually experience ionospheric diffractive effect, which is frequency-independent and immune to the removal by IF combination. Apart from the resultant noisy carrier-phase measurements, small cycle-slips are found in considerable numbers, degenerating the performance of PPP [7]. It is essential to build up an approach that corrects cycle-slips and minimizes the distortion of the diffractive effect to ensure an adequate number of qualified measurements for a well-performed PPP solution satisfying different ionospheric conditions.

First, there are several approaches which have been being widely used to detect cycle-slips [8]. The most robust methodology is based on the geometry-free (GF) combination, denoted L_{GF}. Another detecting approach applying the Melbourne-Wübbena combination [6] has also been used along with the GF combination detector to avoid errors of omission. In quiet ionosphere condition, L_{GF} varies slowly and smoothly with very low noise. Sudden changes or jumps found in L_{GF} are identified as cycle-slips. L_{GF} may fluctuate rapidly with noise amplified as large as cycle-slips, leading to potential false detections of cycle-slips when facing ionospheric scintillation

effects. Alternatively, increasing the false-alarm threshold in GF combination detector may miss-detect small cycle-slips which occur commonly as a result of diffractive scintillation. GF combination detector cannot offer a reliable solution to correct the detected cycle-slips since the combination values significantly vary over time. In order to identify and repair the cycle-slips properly, cycle-slips have to be isolated from the severely fluctuating scintillation effects in the signals.

Second, ionospheric scintillation is characterized using two scintillation indices provided by Ionospheric Scintillation Monitoring Receiver (ISMR): amplitude scintillation index S_4, and phase scintillation index σ_{φ_f} [9]. However, costly ISMRs require the ultra-low-noise Oven-Controlled Crystal Oscillators, which are more precise and stable than the internal clocks of conventional geodetic receivers equipped in most stations of IGS network [1]. A common indicator of scintillation using such geodetic receivers is known as Rate of Total electron content Index (ROTI) [10]. Nonetheless, the contamination of miss-detected cycle-slips in ROTI is one of the drawbacks of this approach. Recently, a novel scintillation index, called $\sigma_{\varphi_{IF}}$, has been proposed and proved to be directly associated to the noise of the IF combination measurements [11]. IF combination is also capable of determining the numbers of cycle-slips, the largest fluctuation due to refractive scintillation has been diminished and the diffractive noise is lower than the cycle-slips.

In this paper we propose a solution for PPP which can correct cycle-slips and discard measurements under diffractive ionospheric scintillation as the aforesaid requirements. This solution applies a geodetic detrending algorithm including receiver clock fluctuation removal and cycle-slips correction [12] to achieve a satellite discarding mask of $\sigma_{\varphi_{IF}}$, named Sigma-IF mask, and a cycle-slips alignment so as to improve the performance and the integrity of the PPP. We detail it in the methodology in Section 2 and 3. Section 4 describes the dataset used in the experiment. Section 5 demonstrates the results of PPP using Sigma-IF-mask in different scenarios. Finally, Section 6 summarizes and presents the conclusions of the proposed approach.

2. Geodetic Detrending Models

In the section, we describe models of observed measurements and their applied linear combinations as introduced in [12] for a geodetic detrending method.

2.1. Models in Dual Frequency PPP

The carrier-phase L_f observed by the receiver at frequency f of each satellite can be modelled as [6]:

$$
\begin{aligned}
L_f^s = \rho^s + \delta_{ant}^s + \delta_{tide}^s + \delta t_u + \delta t^s + Tr^s \\
+ I_f^{s,r} + I_f^{s,d} + w_f^s \\
+ \left(B_f^s + \lambda_f N_f^s\right) + \varepsilon_f^s
\end{aligned} \tag{1}
$$

where ρ is the geometric range from the satellite to the receiver, δ_{ant}^s is the effect caused by Phase Centre Variations of the satellite and the receiver, δ_{tide}^s is the solid tides effect, δt_u and δt^s are effects of the receiver and the satellite clock offsets, Tr^s is the tropospheric delay, $I_f^{s,r}$ and $I_f^{s,d}$ are the ionospheric refractive and diffractive effects, w_f^s is the phase wind-up effect, and the phase ambiguity includes a constant initial real valued offset B_f^s and an integer number N_f^s of cycles bias with wavelength λ_f. ε_f^s is the sum of unmodelled effects of the carrier-phase observables including the measurement noise and the multipath effect.

In the criteria of PPP, the performance requires highly accurate correction models for the aforementioned effects. The first step of both PPP and the proposed Sigma-IF mask is applying these well-known measurement models to determine effects such as δ_{ant}^s, δ_{tide}^s, w_f^s, δt^s and Tr^s. The geometric range ρ^s can be estimated with the approximate coordinates of the static receiver and the satellite, retaining a geometric range mismodelling error denoted as $\delta\rho^s$. After subtracting these PPP-level accurate models from L_f^s in (1), the residual consists of the receiver clock offset effect δt_u, phase ambiguity $\left(B_f^s + \lambda_f N_f^s\right)$, ionospheric effects $\left(I_f^{s,r} + I_f^{s,d}\right)$, together with geometric range mismodelling error $\delta\rho^s$ as follows:

$$
\begin{aligned}
\hat{r}_{L_f}^s = I_f^{s,r} + I_f^{s,d} + \delta\rho^s + \delta t_u \\
+ \left(B_f^s + \lambda_f N_f^s\right)
\end{aligned} \tag{2}
$$

Table 1. IGS products

Product	Parameters	Accuracy	Latency
Ultra-rapid (Predicted)	Orbits	5 cm	Real-time
	Clocks	3 ns	
Rapid	Orbits	2.5 cm	17 - 41 hours
	Clocks	$75 \cdot 10^{-3}$ ns	
Final	Orbits	2.5 cm	12 - 18 days
	Clocks	$75 \cdot 10^{-3}$ ns	

The second step is removing the refractive effect using the ionosphere-free (IF) linear combination of two carrier-phase residuals $\hat{r}_{L_1}^s$ and $\hat{r}_{L_2}^s$ at frequencies L_1 and L_2, respectively. Accordingly, the combined effects of phase ambiguity, mismodelled geometric range, receiver clock bias and diffractive ionospheric scintillation remain as follows:

$$\hat{r}_{L_{IF}}^s = \delta\rho^s + \delta t_u + B_{IF}^s + \lambda_1^{IF} N_1^s$$
$$+ \lambda_2^{IF} N_2^s + I_{IF}^{s,d} \tag{3}$$

In PPP solutions, these residuals $\hat{r}_{L_{IF}}^s$ of all satellites are used to establish the navigation equations to achieve the coordinates of the receiver. In Sigma-IF mask computation, $\hat{r}_{L_{IF}}^s$ is detrended to obtain how fluctuating the diffraction effect $I_{IF}^{s,d}$ is. With static receiver, the geometric range mismodelling error $\delta\rho^s$ varies gradually and contributes unremarkable to the rapid fluctuation of $\hat{r}_{L_{IF}}^s$. On the contrary, the unstable receiver clock bias δt_u and the diffraction effect $I_{IF}^{s,d}$ under scintillation are the main source of the high-rate variation of $\hat{r}_{L_{IF}}^s$. Satellites which have no cycle-slips and under gentle or no scintillation shares a similar fluctuation, which is identical to the variation of the receiver clock bias δt_u and can be estimated.

The estimation of the receiver clock fluctuation $\widehat{\delta t_u}$ is carried out in the third step as the integral of its time derivative $\widehat{\delta t_u}$:

$$\widehat{\delta t_u} = \frac{\sum_{s=1}^n \frac{\hat{\dot{r}}_{L_{IF}}^s}{ROTI_s^2}}{\sum_{s=1}^n \frac{1}{ROTI_s^2}} \tag{4}$$

where ROTI is used as an indicator of scintillation and cycle-slip to down-weight $\hat{r}_{L_{IF}}^s$ under such conditions in the average computation of $\widehat{\delta t_u}$. $\hat{\dot{r}}_{L_{IF}}^s$ is the time derivative of $\hat{r}_{L_{IF}}^s$ and can be expressed as follows:

$$\hat{\dot{r}}_{L_{IF}}^s(k) = \dot{I}_{IF}^{s,d}(k) + \delta\dot{t}_u(k) + \lambda_1^{IF}\dot{N}_1^s(k) + \lambda_2^{IF}\dot{N}_2^s(k) \tag{5}$$

where k is the epoch of interest, $\dot{N}_1^s(k)$ and $\dot{N}_2^s(k)$ are the numbers of cycles changing after cycle-slip. After subtracting the receiver clock fluctuation $\widehat{\delta t_u}$ from $\hat{r}_{L_f}^s$ in (2), we obtain another residual, denoted as $\bar{r}_{L_{IF}}^s$:

$$\bar{r}_{L_{IF}}^s = I_{IF}^{s,d} + \delta\rho^s + \bar{B}_{IF} + \lambda_1^{IF} N_1^s + \lambda_2^{IF} N_2^s \tag{6}$$

The remaining cycle-slips are the last challenge to achieve the appropriate indicator of the diffractive ionospheric effect on IF combinations.

2.2. Cycle-Slips

The number of cycles changing in L_1 and L_2 are respectively $\dot{N}_1^s(k)$ and $\dot{N}_2^s(k)$ as the time derivatives of the integer ambiguities N_1^s and N_2^s. When $\dot{N}_1^s(k)$ and $\dot{N}_2^s(k)$ are solved, the cycle-slip-free residual of $\bar{r}_{L_{IF}}^s$ is expected as:

$$r_{L_{IF}}^s(k) = I_{IF}^{s,d}(k) + \delta\rho^s(k) + \bar{B}_{IF}(k)$$
$$+ \lambda_1^{IF} N_1^s(k-1) \tag{7}$$
$$+ \lambda_2^{IF} N_2^s(k-1)$$

In such a case, the integer ambiguities N_1^s and N_2^s are constant over time. Once N_1^s and N_2^s are precisely estimated, as in PPP solution after the convergence period, the measurements from satellite s are used in the navigation equations with a high weight. In contrast, when N_1^s and/or N_2^s change as the cycle-slip, satellite s has to be discarded or down-weighted in the navigation equations to avoid contamination in the solution. After that, its ambiguities N_1^s and N_2^s are recalculated in a new arc until convergence. It is feasible to detect large and medium cycle-slips using simultaneously the GF combination and the Melbourne-Wübbena combination [6] of L_1 and L_2. Applying such detectors declare a cycle-slip at a satellite and create a new computation arc. Consequently, the detected and down-weighted satellite may downgrade the geometry distribution of satellites.

3. Proposed Methodology

In the proposed method, the two detectors are applied with the thresholds greater than 10 times of the wavelength so only large detected jumps would bring about the creation of a new computation arc. A cycle-slip corrector is applied in order to maintain the phase ambiguity computation arc. The proposed Sigma-IF mask to discard satellites under diffractive ionospheric scintillation is then calculated.

3.1. Cycle-Slip Correction

The cycle-slip correction based on IF combination is implemented as the following steps.

(a) The threshold to declare a cycle-slip in the IF combination is set as 20cm, which is greater than the amplitude of moderate scintillation effect in the IF combination. Specifically, $\bar{r}_{L_{IF}}^s$ at epoch k is predicted as $\widetilde{r_{L_{IF}}^s}(k)$ using the previous values of $\bar{r}_{L_{IF}}^s$. When the difference of the observed $\bar{r}_{L_{IF}}^s(k)$ and the predicted $\widetilde{r_{L_{IF}}^s}(k)$ is larger than 20 cm, a cycle-slip is detected.

(b) $\dot{N}_1^s(k)$ and $\dot{N}_2^s(k)$ are searched in an integer domain, for instance $[-9, 9]$, to fulfill the following conditions:

- The difference of the predicted $\widetilde{r_{L_{IF}}^s}(k)$ and the cycle-slip-free residual $r_{L_{IF}}^s(k)$ after removing the searched values $(|r_{L_{IF}}^s(k) - \widetilde{r_{L_{IF}}^s}(k)|)$ is minimised;

- $|r_{L_{IF}}^s(k) - \widetilde{r_{L_{IF}}^s}(k)|$ is less than 20 cm.

In case the obtained $|r_{L_{IF}}^s(k) - \widetilde{r_{L_{IF}}^s}(k)|$ is greater than 20 cm, the cycle-slip is declared as detected but uncorrected and a new computation arc is created. This phenomenon usually occurs in case of severe scintillation when the amplitude of diffractive ionospheric effect in the IF combination is too large to obtain a reliable prediction of $\widetilde{r_{L_{IF}}^s}(k)$.

3.2. Sigma-IF Mask

As introduced in [12], Sigma-IF , denoted as σ_{IF}^s, is the standard deviation over a window of 60 seconds of the detrended IF combination, which is the receiver-clock-and-cycle-slip-free residual $r_{L_{IF}}^s$ in (7).

$$\sigma_{IF}^s = \sigma_{60s}(r_{L_{IF}}^s) \qquad (8)$$

Since the variations of $\delta\rho^s$ and $\bar{B}_{IF}$ are at low rate, high values in the standard deviation of $r_{L_{IF}}^s$ are mostly caused by diffractive scintillation in $I_{IF}^{s,d}$.

In order to discard satellites under scintillation in the navigation equations, a mask based on σ_{IF} is proposed in this method. The threshold of the mask is adaptive to the number of satellites to maintain the adequate distribution. Since the standard deviation of carrier measurement noise is less than 1.46 mm [13], satellites which have σ_{IF}^s less than 6 mm are not scintillating. They are considered to have the most precise carrier phase measurements and to be used in the navigation equations. Other satellites which have greater σ_{IF}^s are discarded. The cycle-slips are detected and corrected in this Sigma-IF masked method.

However, in severe scintillation conditions, the number of fulfilled satellites are limited and can be inadequate to solve the receiver position. When the number of satellites which have σ_{IF}^s less than 6 mm is less than 10, the average number of visible GPS satellites, and other satellites are discarded, the dilution of precision DOP is high and the performance of PPP would decrease. A higher threshold for σ_{IF}^s is recommended for the proposed method in order to increase the number of navigation equations. In the scope of this implement, a threshold of 12 mm is selected by experiments as the optimal one for the Sigma-IF mask in such condition.

4. Dataset

The observables used in this study are collected on day 251 (8th September) of 2017 from COCO00AUS, an IGS station in Cocos (Keeling) Islands. The data is in RINEX format and sampled at 1 Hz. Since the performance of PPP is distorted when the frequencies are affected differently by equatorial scintillation, these observables are used as an example of receiver working at low latitude.

The precise orbits and clocks are provided in the final products and ultra-rapid products from IGS. The result with final products demonstrates the effect of equatorial scintillation on the state-of-the-art PPP and on the proposed method. The result with ultra-rapid products provides the availability and the performance of these methods in a less precise scenario but in real-time latency.

The PPP results are achieved using GNSS-Lab Tool (gLAB) with proposed masks as the input of User Added Error. The tropospheric effects are corrected using the nominal tropospheric delay prediction and the mapping of Niell featured in gLAB. The usage of measurements in the state-of-the-art PPP and proposed methods is described in Table 2.

Table 2. Measurement usage in aforementioned methods

Methods	Measurements with non-ionospheric noise	Measurements with scintillation noise	Measurements with Cycle-slips
Standard PPP	Used	Used	Detected-Discarded
Sigma-GF mask	Discarded	Discarded	Detected-Discarded
Sigma-IF mask with cycle-slip correction	Discarded	Discarded	Corrected

5. Results and Analysis

In quite scintillation condition, since noisy observables are due to non-ionospheric errors, they can be discarded using either Sigma-GF mask or Sigma-IF mask likewise. As a result, both Sigma-GF masked and Sigma-IF masked methods have the similar accuracy in the navigation results in most epochs. As expected, using either mask can enhance the precision of PPP to

a slightly higher level than the standard one without any masks. The adaptive thresholds of both masks help avoid limited number of satellites in use.

Under moderate and strong scintillation as from epoch 45000 to 60000, standard PPP suffers from low precision owing to noisy measurements and several converging peaks caused by cycle-slips. Applying either Sigma-GF mask and Sigma-IF mask improves

significantly the precision of PPP. Indeed, only satellites with low noise are used in the position computation to obtain a smoother solution than in the standard PPP. New satellites participating to the navigation equations usually have noisy measurements due to low elevation and unknown ambiguities causing high converging peaks. Sigma-GF mask method can reduce or totally remove such peaks by discarding noisy satellites. In Sigma-GF masked method, satellites detected with cycle-slips are discarded to

remain only measurements with low noise. However, a high number of discarded satellites may cause higher DOP and thus, lower accuracy. On the contrary, Sigma-IF masked method can retain several satellites with cycle-slips by correcting them. Indeed, with less peaks in East-North-Up (ENU) errors of the PPP solution, Sigma-IF masked method uses more satellites to achieve a higher precision than Sigma-GF masked one in most epochs.
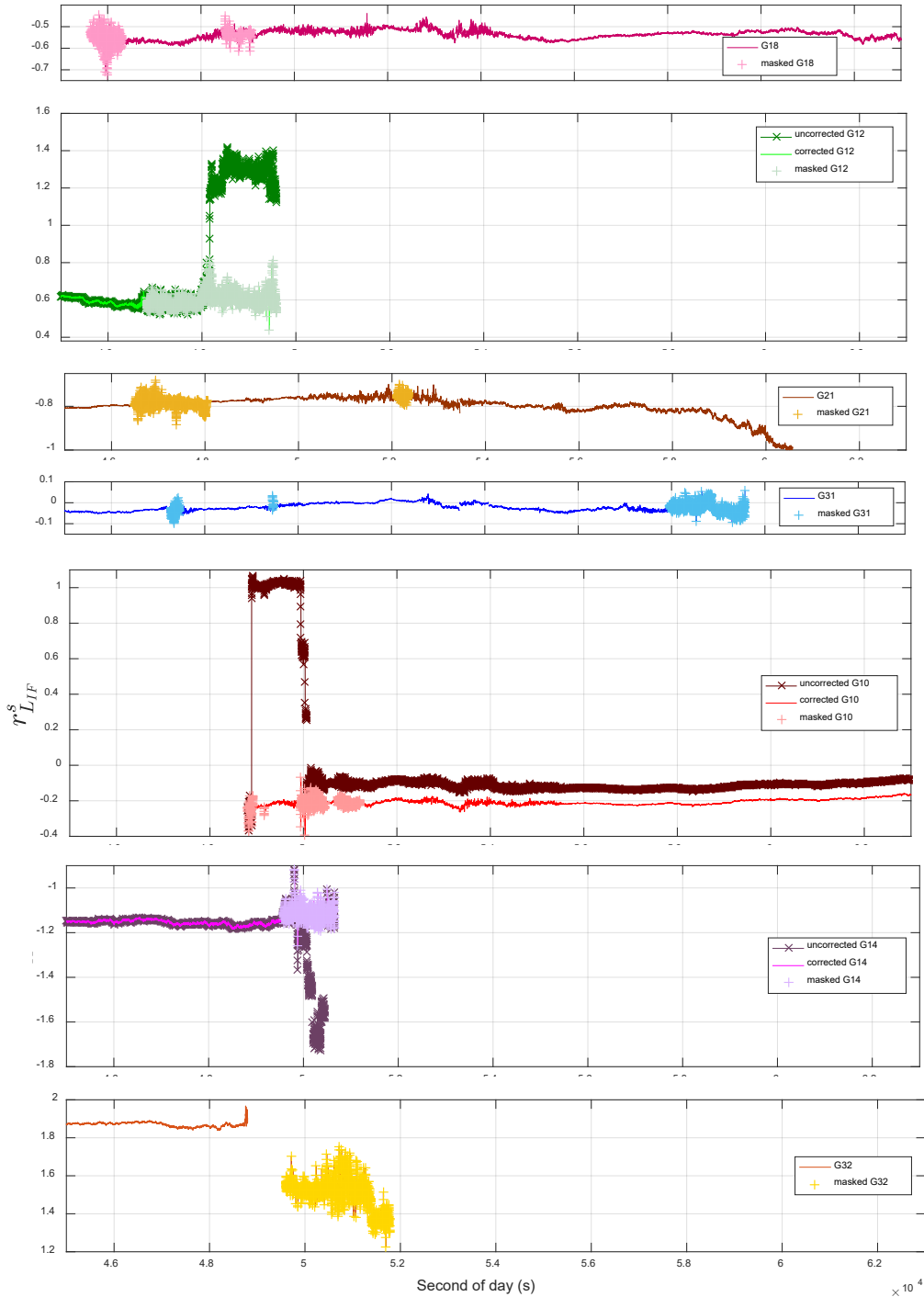

Fig. 1. Detrended residuals $r_{L_{IF}}^s$ of satellites in view during scintillation at COCO00AUS with and without cycle-slip correction, and masked periods determined by the proposed Sigma-IF mask.

The G18 subject to scintillation as the fluctuating $r_{L_{IF}}^{G18}$ in Fig. 1 from epochs 45639s to 46301s leads to low precision in ENU errors of the plain PPP solution.

On the contrary, measurements of G18 in this period is masked in the Sigma-IF masked solution. As a result, PPP with Sigma-IF mask is improved in the precision of all ENU errors, as seen in Fig. 2.
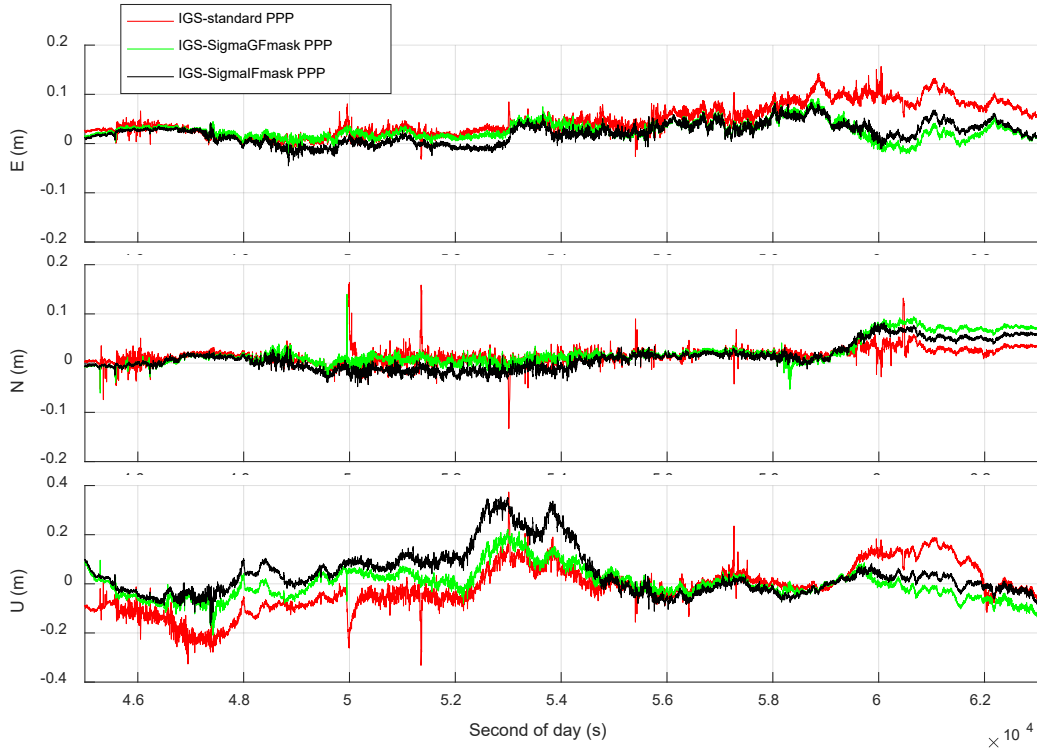
(a) under scintillation condition
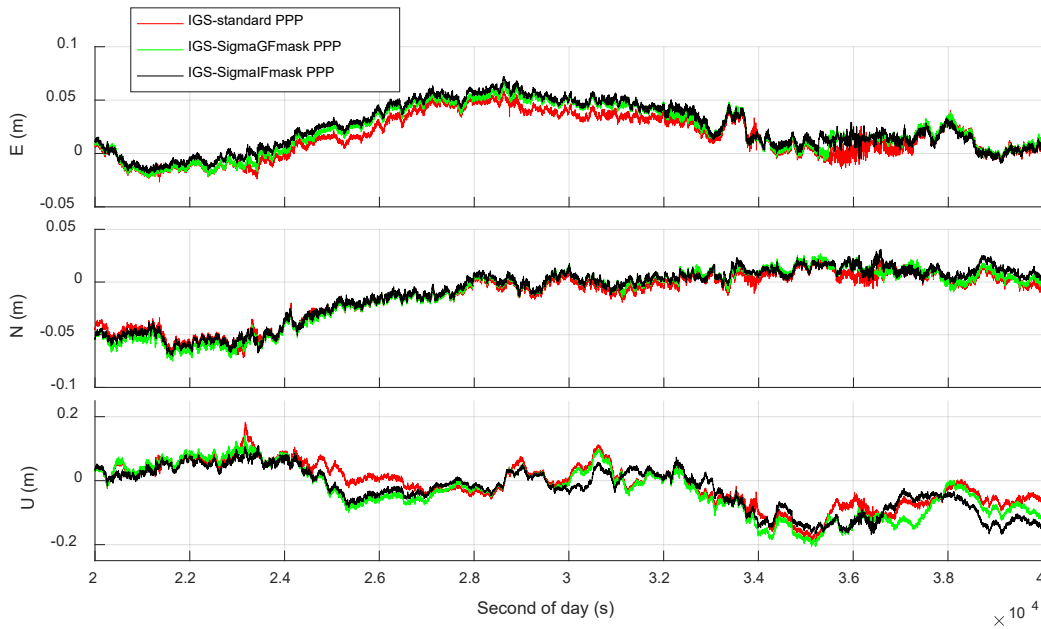
(b) under moderate condition

Fig. 2. East-North-Up errors of the 3 solutions: standard PPP, PPP using Sigma-GF mask, PPP using Sigma-IF mask with precise orbits and clocks from IGS Final products.
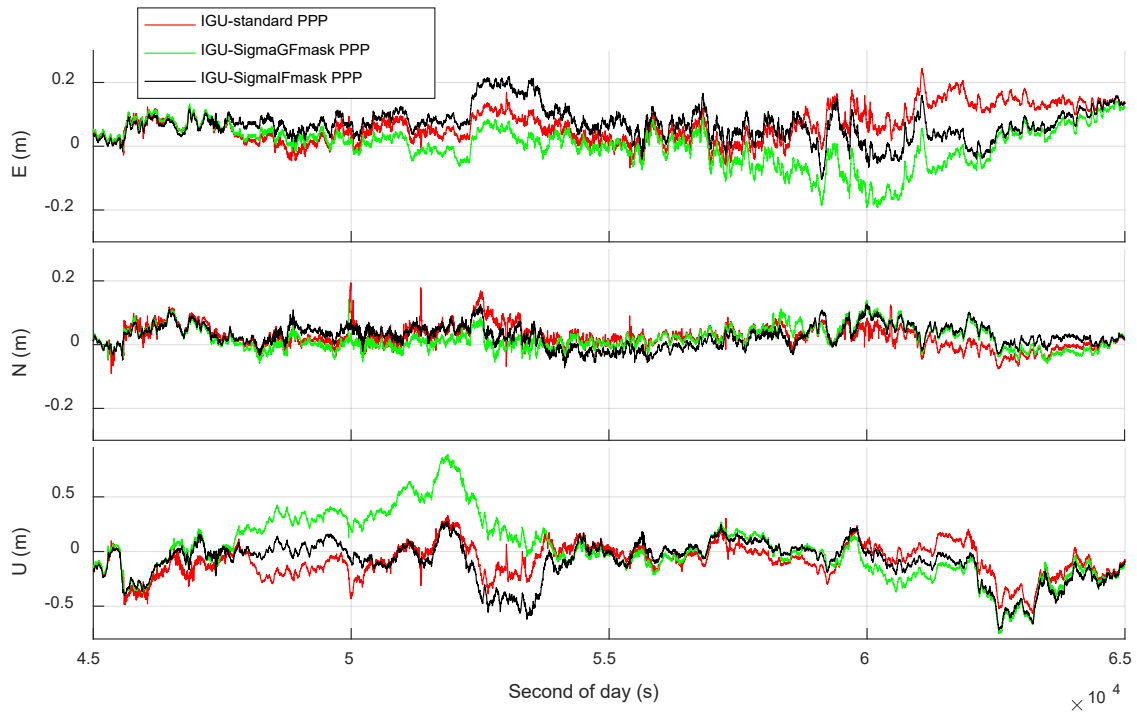
Fig. 3. East-North-Up errors of the 3 solutions: standard PPP, PPP using Sigma-GF mask, PPP using Sigma-IF mask with precise orbits and clocks from IGS Ultra-Rapid products.

Table 3. Standard deviations of the East-North-Up errors of aforementioned methods

Periods	Standard PPP	Sigma-GF mask	Sigma-IF mask with cycle-slip correction
20000s to 40000s (moderate)	3.8 mm	3.6 mm	3.6 mm
45000s to 60000s (scintillation)	9.8 mm	6.5 mm	6.5 mm

Similarly, scintillating measurements of G21 from 46503s to 48048s, of G31 from 47273s to 47462s, and of G12 from 46824s to 49586s experiencing high Sigma-IF are masked. Applying this discarding method slightly improves the precision of the Up error. A cycle-slip of G12 occurs at epoch 48166 is detected by both plain PPP solution and PPP with Sigma-GF mask. In those solutions, G12 are reset after the cycle-slip and its participation in the navigation equations is downweighted in the initial stage. In PPP with Sigma-IF mask, G12 measurements after the cycle-slip are totally discarded even with a correction since its Sigma-IF values are over the threshold. Therefore, the precision of all three solutions after the cycle-slip of G12 at epoch 48166 are similar until epoch 49579 when scintillation is getting severe in several satellites such as G10, G14 and G32.

Following up on the Sigma-IF masked method, the measurements of G10, G14 and G32 from epoch 49579 to 51775, which are suffering from cycle-slips and scintillation, are corrected or masked. A

remarkable improvement is obtained in the proposed Sigma-IF masked method during this period. Both Sigma-GF masked and Sigma-IF masked solutions diminish the noise of the ENU errors after discarding measurements with high scintillation indices. However, the cycle-slip of G10 at 49948 is miss-detected by both plain PPP and Sigma-GF masked solutions causing incorrect ambiguity resolution and consequent high values in their ENU errors. Thanks to cycle-slip correction, Sigma-IF masked method eliminates high peaks due to resetting arcs of computation including ambiguity resolution resets. Analogously, the discarding of scintillating G31 starting from epoch 57961 to 60584 helps improving the precision of Sigma-IF masked and Sigma-GF masked PPP solutions comparing with the state-of-the-art PPP solution.

The improvement in precision is also achieved in the scenario using precise orbits and clocks from IGS Ultra-Rapid products. As expected, high peaks of convergence are significantly reduced in Sigma-GF

mask method and completely removed in the Sigma-IF mask one. The limitation of satellite numbers in Sigma-GF mask method causes biases in its solution, noticeably seen in the Up errors. The Sigma-IF mask method enhances the precision. However, the general accuracy of the three solutions: standard PPP, PPP using Sigma-GF mask, and PPP using Sigma-IF mask are similar.

6. Conclusion

The Sigma-IF mask based on detrended residuals of the linear ionosphere-free (IF) combinations of dual-frequency carrier-phased measurements is proposed in order to enhance the state-of-the-art PPP solution for static receivers during diffractive scintillation. Since PPP solutions are distorted by ionospheric diffraction, which occurs frequently in low latitude regions, rather ionospheric refraction, the Sigma-IF mask is compared with another masking method (Sigma-GF) based on the geometry-free (GF) combination which performs under diffractive scintillation and refractive scintillation similarly. The analysis in the result section demonstrates that both Sigma-IF and Sigma-GF significantly improve the precision and the accuracy of the PPP solution from 15 cm to less than 5 cm when using the final orbits and clocks from IGS in severe diffractive scintillation condition. Results with improved precision when applying the ultra-rapid orbits and clocks exhibits the possibility of a real-time scenario.

The cycle-slip correction based on detrended IF combination contributes an important part in the outperformance of the proposed method as high peaks of inaccuracy due to discontinued ambiguity solutions are diminished.

7. Acknowledgments

References

[1] G. Johnston, A. Riddell, G. Hausler, The International GNSS Service, Springer Handbook of Global Navigation Satellite Systems, P. J. Teunissen and O. Montenbruck, Eds., Cham, Springer International Publishing, 2017, pp. 967-982, http://dx.doi.org/10.1007/978-3-319-42928-1_33.

[2] Automatic Precise Positioning Service (APPS), [Online], https://apps.gdgps.net/.

[3] J. M. Juan, J. Sanz, G. González-Casado, A. Rovira-Garcia, Feasibility of precise navigation in high and low latitude regions under scintillation conditions, J. of Space Weather and Space Climate, vol. 8, p. A05, 2018, https://doi.org/10.1051/swsc/2017047.

[4] S. Skone, M. Feng, F. Ghafoori, R. Tiwari, Investigation of scintillation characteristics for high latitude phenomena, Proc. of the 21st International Technical Meeting of the Satellite Division of The Institute of Navigation (ION GNSS 2008), Savannah, GA (USA), 2008.

[5] J. F. Zumberge, M. B. Heflin, D. C. Jefferson, M. M. Watkins, F. H. Webb, Precise point positioning for the efficient and robust analysis of GPS data from large networks, Journal of Geophysical Research: Solid Earth, vol. 102, pp. 5005-5017, 1997, https://doi.org/10.1029/96JB03860.

[6] J. Sanz Subirana, M. Hernández-Pajares and J. M. Juan Zornoza, GNSS Data Processing, Vol. I: Fundamentals and Algorithms, ESA Communications, 2013.

[7] Y. Béniguel, V. Romano, L. Alfonsi, M. Aquino, Ionospheric scintillation monitoring and modeling, Annals of Geophysics, vol. 52, pp. 3-4, 2009, http://dx.doi.org/10.4401/ag-4595.

[8] W. Liu, X. Jin, M. Wu, J. H, Y. Wu, A new real-time cycle slip detection and repair method under high ionospheric activity for a triple-frequency GPS/BDS receiver, Sensors (Basel, Switzerland), vol. 18, no. 2, p. 427, 2018, http://dx.doi.org/10.3390/s18020427.

[9] Zhao, D., Li, W., Li, C., Tang, X., Wang, Q., Hancock, C. M., *et al*, Ionospheric phase scintillation index estimation based on 1 Hz geodetic GNSS receiver measurements by using continuous wavelet transform, Space Weather, 20, e2021SW003015, 2022, https://doi.org/10.1029/2021SW003015

[10] Dongsheng Zhao, Wang Li, Chendong Li, Craig M. Hancock, Gethin Wyn Roberts, Qianxin Wang, Analysis on the ionospheric scintillation monitoring performance of ROTI extracted from GNSS observations in high-latitude regions, Advances in Space Research, vol. 69, no. 1, 2022, p. 142-158, https://doi.org/10.1016/j.asr.2021.09.026.

[11] J. M. Juan, A. Aragon-Angel, J. Sanz, G. González-Casado, A. Rovira-Garcia, A method for scintillation characterization using geodetic receiver operating at 1Hz, J. of Geodesy, vol. 91, no. 11, p. 1383–1397, 2017, http://dx.doi.org/10.1007/s00190-017-1031-0.

[12] V. K. Nguyen, A. Rovira-Garcia, J. M. Juan, J. Sanz, T. V. La, T. H. Ta, Measuring phase scintillation at different frequencies with conventional GNSS receivers operating at 1 Hz, Journal of Geodesy, no. 93, 2019, http://dx.doi.org/10.1007/s00190-019-01297-z.

[13] K. Kazmierski, T. Hadas, K. Sośnica, Weighting of multi-GNSS observations in real-time precise point positioning, Remote Sensing, vol. 10, no. 1, p. 84, 2018, https://doi.org/10.3390/rs10010084